

# Uncertainties in estimating the roughness coefficient of rock fracture surfaces

Yanrong Li<sup>1</sup>  · Qiang Xu<sup>2</sup> · Adnan Aydin<sup>3</sup>

Received: 1 February 2016 / Accepted: 19 December 2016 / Published online: 30 December 2016  
© Springer-Verlag Berlin Heidelberg 2016

**Abstract** Joint roughness has a critical role in the deformation behavior of discontinuous rock masses. Several subjective (visual comparison) and quantitative (statistical and fractal) approaches have been proposed for estimating rock joint roughness coefficient (JRC). Using a large collection of 223 published joint profiles, this study investigates variability of the JRC estimates by these approaches. Among the profile parameters, maximum height ( $R_z$ ), ultimate slope ( $\lambda$ ), and fractal dimension ( $D_{h-L}$ , determined using the hypotenuse leg method) show a lower sensitivity to the sampling interval than the root mean square of the first deviation ( $Z_2$ ), profile elongation index ( $\delta$ ), fractal dimension ( $D_c$ , determined using the compass-walking method), and standard deviation of the angle  $i$  ( $\sigma_i$ ). Accordingly, this study proposes two separate sets of equations for quantitatively estimating JRC. The performances of these equations are examined by performing direct shear tests on 23 rock joint samples. The subjective approach is found to underestimate JRC by less than two units because it ignores (1) the main trend of the compared profile and (2) the limited scope of the standard profiles. Following these results, the visual

comparison chart is updated by explicitly adding a scale bar for the y-axes of the standard profiles. Several basic rules for visual comparisons are also proposed.

**Keywords** JRC estimation · Visual comparison · Empirical equation · Sampling interval

## Abbreviations

$Z_2$	Root mean square of the first deviation of the profile
SF	Structure function of the profile
$\sigma_i$	Standard deviation of the angle $i$
$R_z$	Maximum height of the profile
$L$	Projected length of the profile
$L_t$	Total length of the profile
$\lambda$	Ultimate slope of the profile
$\delta$	Profile elongation index
$D$	Fractal dimension of the profile
$D_c$	Fractal dimension determined via compass-walking method
$D_{h-L}$	Fractal dimension determined via hypotenuse leg (h-L) method
SI	Sampling interval
$\theta_{max}^*$	Maximum apparent asperity inclination
JRC	Joint roughness coefficient
JRC <sub>v</sub>	JRC estimated via visual comparison
JRC <sub>e</sub>	JRC estimated via quantitative method
$\gamma$	Deviation of JRC <sub>v</sub> from JRC <sub>e</sub> ( $\gamma = JRC_v - JRC_e$ )

✉ Yanrong Li  
li.dennis@hotmail.com

Qiang Xu  
xq@cdut.edu.cn

Adnan Aydin  
aaydin@olemiss.edu

<sup>1</sup> Taiyuan University of Technology, Taiyuan 030024, China

<sup>2</sup> State Key Laboratory of Geohazard Prevention and Geoenvironment Protection, Chengdu University of Technology, Chengdu 610059, China

<sup>3</sup> Department of Geology and Geological Engineering, University of Mississippi, Oxford, MS 38677, USA

## Introduction

Since Barton (1973) introduced the joint roughness coefficient-joint compressive strength (JRC-JCS) model for determining the peak shear strength of a rock joint and

developed a subjective method for estimating the JRC of rock joints (Barton 1973; Barton and Choubey 1977), many quantitative (Tse and Cruden 1979; Yu and Vayssade 1991; Kulatilake et al. 1995; Grasselli and Egger 2003; Tatone 2009; Tatone and Grasselli 2010, 2013; Gao and Wong 2015) methods have been proposed. Recommended by the International Society for Rock Mechanics (ISRM) (Brown 1981), the subjective method (Barton and Choubey 1977) estimates JRC by visually comparing a rock joint profile with 10 standard profiles whose JRC values range from 0 to 20. Despite its efficiency, this method often introduces errors or variations in that the user has to match the profiles subjectively. By contrast, quantitative approaches minimize errors and avoid subjectivity by considering statistical parameters and the fractal dimension. Representative statistical parameters include the root mean square of the first deviation of a profile ( $Z_2$ ), structure function of a profile (SF), standard deviation of the angle  $i$  ( $\sigma_i$ ), profile elongation index ( $\delta$ ), angular threshold ( $\theta_{\max}^*$ ), and roughness index (Yang et al. 2001; Maerz et al. 1990; Wang 1982; Tatone and Grasselli 2010, 2013; Zhang et al. 2014). The fractal dimension ( $D$ ) has a variety of definitions, which employ different approaches to determine it as a roughness parameter (Turk et al. 1987; Carr and Warriner 1987; Lee et al. 1990; Xie and Pariseau 1994).

Difficulties are often encountered when ranking the suitability of these equations for use in engineering practice. Li and Zhang (2015) carried out a review of quantitative estimates of JRC by statistical parameters, reformatted the terms and symbols in previously published equations according to international standards, and discussed the limitations of each equation. Based on a large collection of published rock joint profiles, Li and Zhang (2015) proposed a new set of empirical equations that could improve the correlations of JRC with the maximum height ( $R_z$ ), ultimate slope ( $\lambda$ ), and elongation index ( $\delta$ ) of the joint profile.

A similar review was also made by Li and Huang (2015) for the correlations between JRC and  $D$  of joint profiles. They found that the limited number of data points and the inconsistency in the approaches employed in the literature for determining  $D$  introduced huge variations among the previously published equations. The 10 standard profiles on which most equations proposed in the literature have been based were insufficient for deriving a reliable correlation between JRC and  $D$ . Different  $D$ -determination methods [i.e., compass-walking, box-counting, and hypotenuse leg (h–L)] may produce very different  $D$  values for a certain profile. Li and Huang (2015) proposed new empirical equations that suggested a close relationship between JRC and  $D$  from the compass-walking and updated h–L methods. However, the  $D$  value estimated using the box-counting method did not correlate as well with JRC. The

updated h–L method was recommended for use in engineering practice because of its easy application and strong correlation with JRC.

On the other hand, the sampling interval (SI) used in the digitization of profiles may influence the values of roughness parameters. Yu and Vayssade (1991) discussed the SI-induced variations when using  $Z_2$ ,  $\sigma_i$ , and SF in estimating JRC, and found that the correlations demonstrated a rightward shift with finer SI as indicated by the thick gray arrow in Fig. 1. Tatone and Grasselli (2010) found that the correlations between JRC and  $Z_2$  were sensitive to SI. Therefore, different equations must be used for different SIs.

To understand further the influence of SI, this study retrieved 112 joint profiles (for which the JRC values were originally determined through the back calculation of direct shear tests) from the literature and digitized them with SIs ranging from 0.1 to 3.2 mm. The dependence of the quantitative correlations on SI was examined, and a new set of correlations that consider SI was proposed. The proposed equations were tested by performing direct shear tests on 23 rock joint samples. An additional set of 111 rock joint profiles (for which JRC values were originally determined via visual comparison) was compiled from the literature to investigate the deviations of the JRC values estimated via visual comparison ( $JRC_v$ ) from those estimated using empirical equations ( $JRC_e$ ).

## Data preparation

This study makes use of 223 published rock joint profiles, JRC values of which were determined by the original researchers. These profiles are then divided into two sets. The first set, which includes 112 profiles, is used to investigate the influence of SI. The JRC values of these profiles were determined in the literature by back calculation from direct shear test results. In addition to the 10 standard profiles, this first set contains 12, 26, and 64 profiles taken from Grasselli (2001), Bandis et al. (1983) and Bandis (1980), respectively. The second set, which includes 111 profiles, is used to investigate the uncertainties in visual comparison. The JRC values of these rock joint profiles were determined via visual comparison in the literature. The subsets of these profiles are borrowed from various sources: nine profiles from Du (1995), three from Beer et al. (2002), 24 from Seidel and Haberfield (1995), 12 from Grasselli (2001), four from Vladimir and Tomas (2011), eight from Herda (2006), eight from Rasouli and Hosseini (2011), 42 from Jia (2011), and one from Odling (1994).

The 223 profiles have projected lengths ranging from 68 to 167.8 mm and the JRC values ranging from 0.4 to 20.0

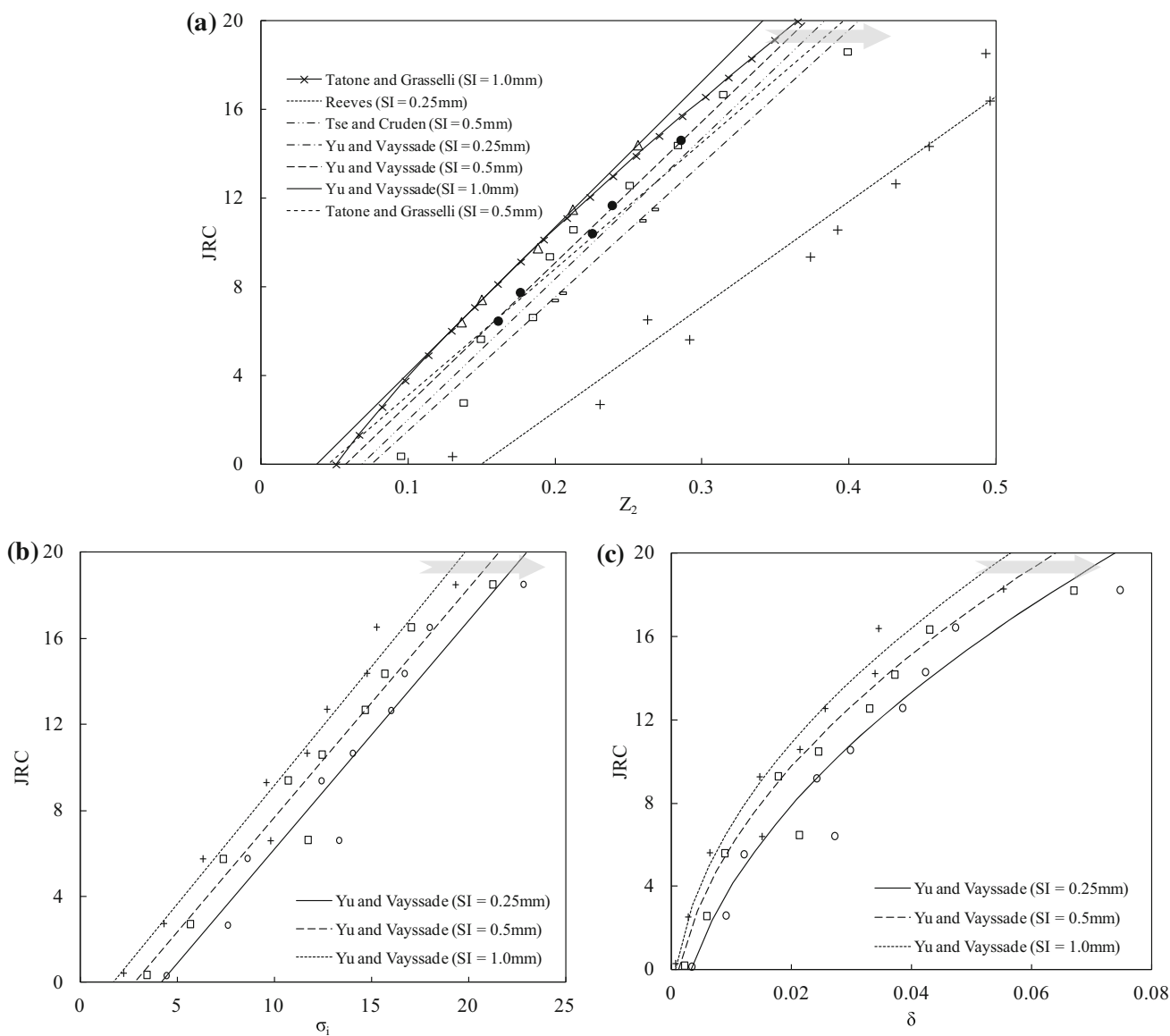


**Fig. 1** Dependence of degree of correlations between JRC and some statistical parameters ( $Z_2$ ,  $\sigma_i$ ,  $\delta$ ) on the sampling interval, SI (the thick gray arrow indicates the decrease in SI)

as reported in the literature. These joint profiles represent a wide variety of rocks, including sandstone, limestone, marble, granite, gneiss, slate, dolerite, and siltstone, with various weathering degrees (fresh, slight, and moderate). These profiles range from well-interlocked planar cleavage surfaces to poorly-interlocked and rough walls.

Given the lack of digital data, the images of these profiles as presented in the original publications are imported into AutoCAD. The dimension setting of AutoCAD is adjusted for each image according to the scale bar on the original figure. The first set of 112 profiles are digitized at SIs of 0.1, 0.2, 0.4, 0.8, 1.6, and 3.2 mm, while a constant SI of 0.4 mm is used for the profiles in the second set.

During the digitization process, a set of vertical lines is constructed at each SIs across the length of the profiles. A polyline is created by connecting the intersections of the vertical lines with the profile. The polylines are then imported into a computer program developed by the authors to calculate the statistical parameters and  $D$  of the profiles. This digitization process avoids the undesirable thickness encountered by Gao and Wong (2015) who employed the pixel analysis method to digitize the 10 standard profiles.

Despite great care taken in processing the data, some minor errors cannot be avoided because the joint profiles are essentially re-sampled from the literature.

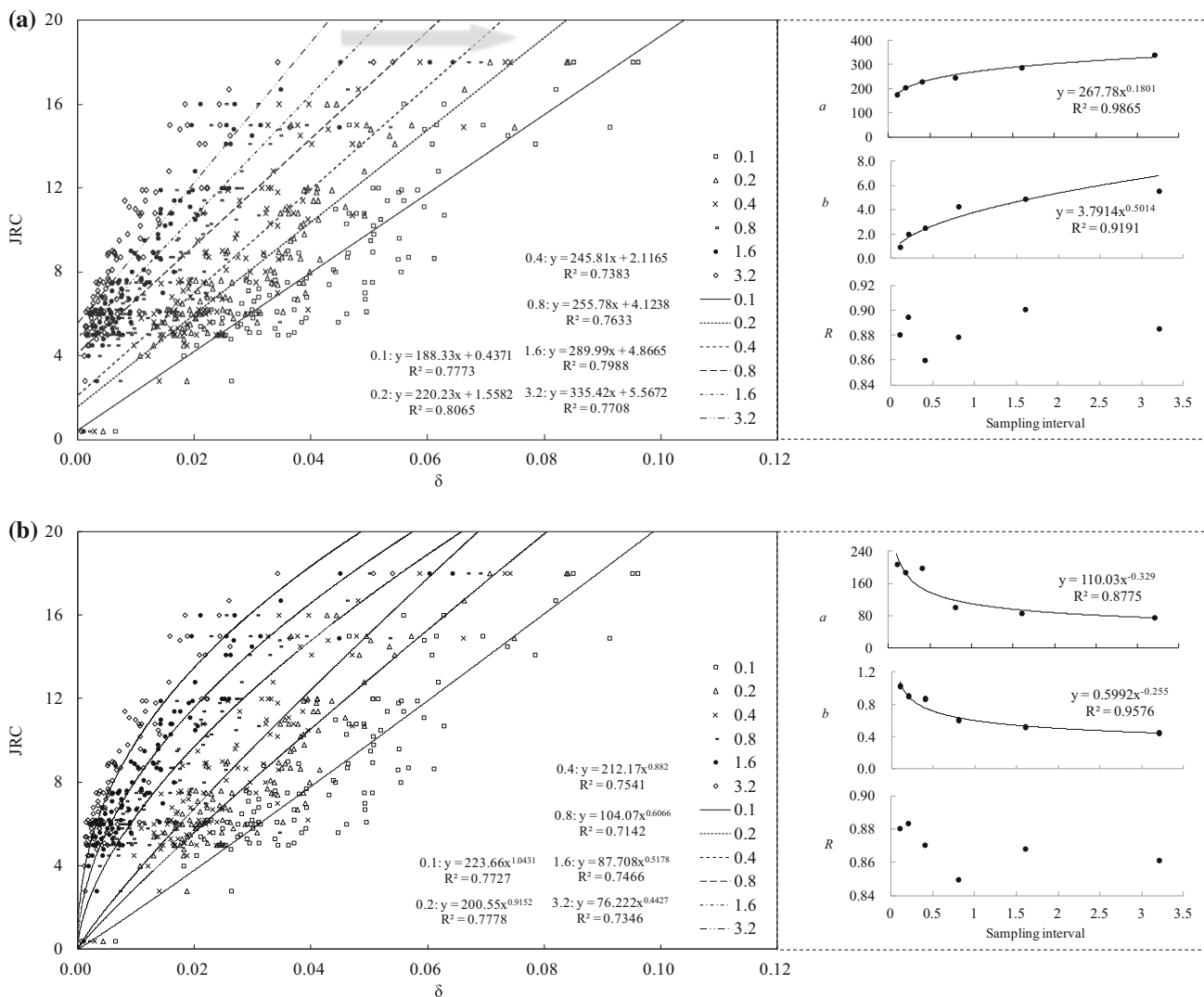


**Fig. 2** Influence of the sampling interval on  $\delta$ -estimates of JRC: **a** linear ( $y = ax + b$ ); and **b** power-law ( $y = ax^b$ ) correlations. To the right is the change of  $a$ ,  $b$  and  $R$  with sampling interval, where  $a$  and  $b$  are the coefficients of regression, and  $R$  is the correlation coefficient

**Results and discussion**

**Influence of SI**

According to Li and Huang (2015) and Li and Zhang (2015), seven parameters, including  $\delta$ ,  $\sigma_i$ ,  $Z_2$ ,  $D_c$ ,  $\lambda$ ,  $R_z$ , and  $D_{h-L}$ , can estimate the JRC of rock joints because of their close linear and/or power-law correlations with JRC. Accordingly, these parameters were calculated for each profile in the first set from the digitized data. The definition and calculation of these parameters are presented in the “Appendix”.

The parameters  $\delta$ ,  $\sigma_i$ ,  $Z_2$ , and  $D_c$  are all closely correlated with JRC (Figs. 2, 3, 4). Generally, a higher value of these parameters indicates a rougher joint surface or higher JRC. These parameters are also found to be sensitive to SI. As shown in Fig. 2, with the decrease in SI (as indicated by

the thick gray arrow), the correlation between JRC and  $\delta$  shifts towards the right and gets gentler. The constants  $a$  and  $b$  increase along with SI for the linear ( $y = ax + b$ ) correlations (Fig. 2a), but decrease for the nonlinear (power-law,  $y = ax^b$ ) regression (Fig. 2b). The correlation coefficient  $R$  shows no dependence on SI. As shown in the “Appendix”,  $\delta$  is equivalent to the ratio of  $L_t - L$  to  $L$ . For an irregular curve, a finer SI corresponds to a longer total length  $L_t$ , while an unchanged projected length  $L$  results in a larger  $\delta$ . The parameter  $\sigma_i$  behaves approximately the same as  $\delta$  as shown in Fig. 3. Similarly, both  $Z_2$  (Fig. 4a, b) and  $D_c$  (Fig. 4c, d) show strong sensitivity to SI.

Given the influence of SI on the quantitative estimation of JRC, a multivariable regression is performed by taking  $\delta$  or  $\sigma_i$  and SI as the independent variables. This produces the following relationships with high correlation coefficients:

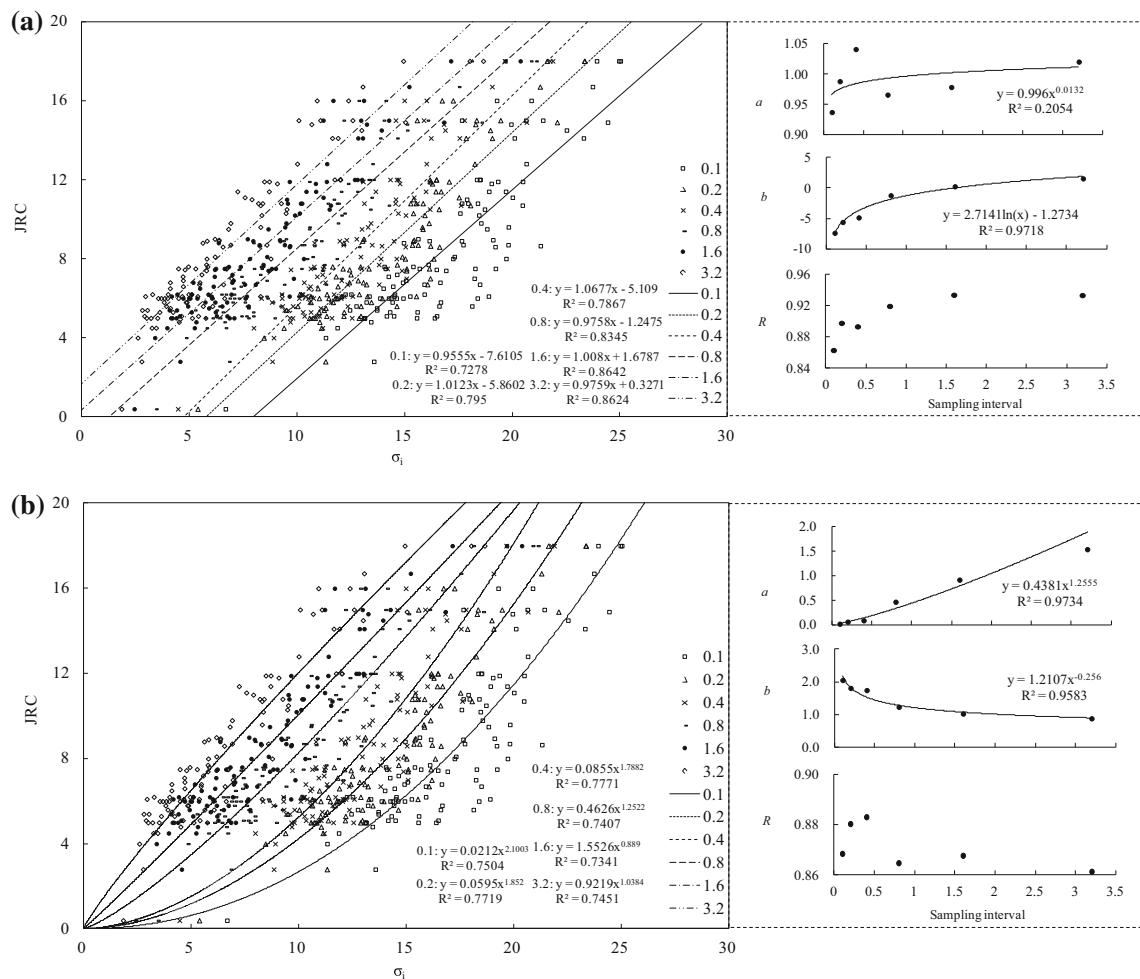


**Fig. 3** Influence of the sampling interval on  $\sigma_f$ -estimates of JRC: **a** linear ( $y = ax + b$ ) and **b** power-law ( $y = ax^b$ ) correlations. To the right is the change of  $a$ ,  $b$ , and  $R$  with sampling interval, where  $a$  and  $b$  are the coefficients of regression, and  $R$  is the correlation coefficient

$$JRC = a\delta^b - 0.2256$$

where,  $\begin{cases} a = 87.142 SI^{-0.2209} \\ b = 0.5382 SI^{-0.2212} \end{cases} (R = 0.8956)$  (1)

$$JRC = a\sigma_f^b - 1.0066$$

where,  $\begin{cases} a = 0.9345 SI^{0.5408} \\ b = 1.0104 SI^{-0.1041} \end{cases} (R = 0.8813)$  (2)

$Z_2$  and  $D_c$  are also examined in a multivariable regression with SI as the second variable, which produces no favorable relationships ( $R < 0.5$ ) with JRC because of their small ranges. Note that  $Z_2$  ranges from 0 to 0.5 for most rock fractures, while  $D_c$  begins from 1.0 for a smooth fracture and can rarely go beyond 1.05 for a very rough fracture.

Figure 5 shows that  $\lambda$ ,  $R_z$ , and  $D_{h-L}$  are hardly sensitive to SI because  $R_z$  represents the maximum height of the profile and is not strongly dependent on SI,  $\lambda$  is equal to the ratio of  $R_z$  to  $L$  where  $L$  is fixed, and the  $D_{h-L}$  computed

from the valleys and peaks of a profile behaves similarly as  $R_z$ .

As defined in the “Appendix”,  $\delta$ ,  $\sigma_i$ ,  $Z_2$ , and  $D_c$  reflect the overall roughness (both high- and low-order waviness) of a profile, while  $\lambda$ ,  $R_z$ , and  $D_{h-L}$  can only describe the high-order waviness. However, these parameter groups have similar correlation coefficients as shown in Figs. 2, 3, 4, and 5, suggesting that JRC has a closer relationship with high-order waviness than low-order waviness. Therefore,  $\lambda$ ,  $R_z$ , and  $D_{h-L}$  are preferred for estimating JRC because they are much simpler to calculate than  $\delta$ ,  $\sigma_i$ ,  $Z_2$ , and  $D_c$ .

For a planar joint (e.g., a saw-cut profile) with a JRC of zero, the corresponding  $\lambda$ ,  $R_z$  and  $D_{h-L} - 1$  should also be equal to zero. However, the linear correlations in all figures have non-zero JRC values. Therefore, the following power-law correlations are suggested for engineering practice:

$$JRC = 80.37\lambda^{0.6238} (R = 0.8158)$$
 (3)

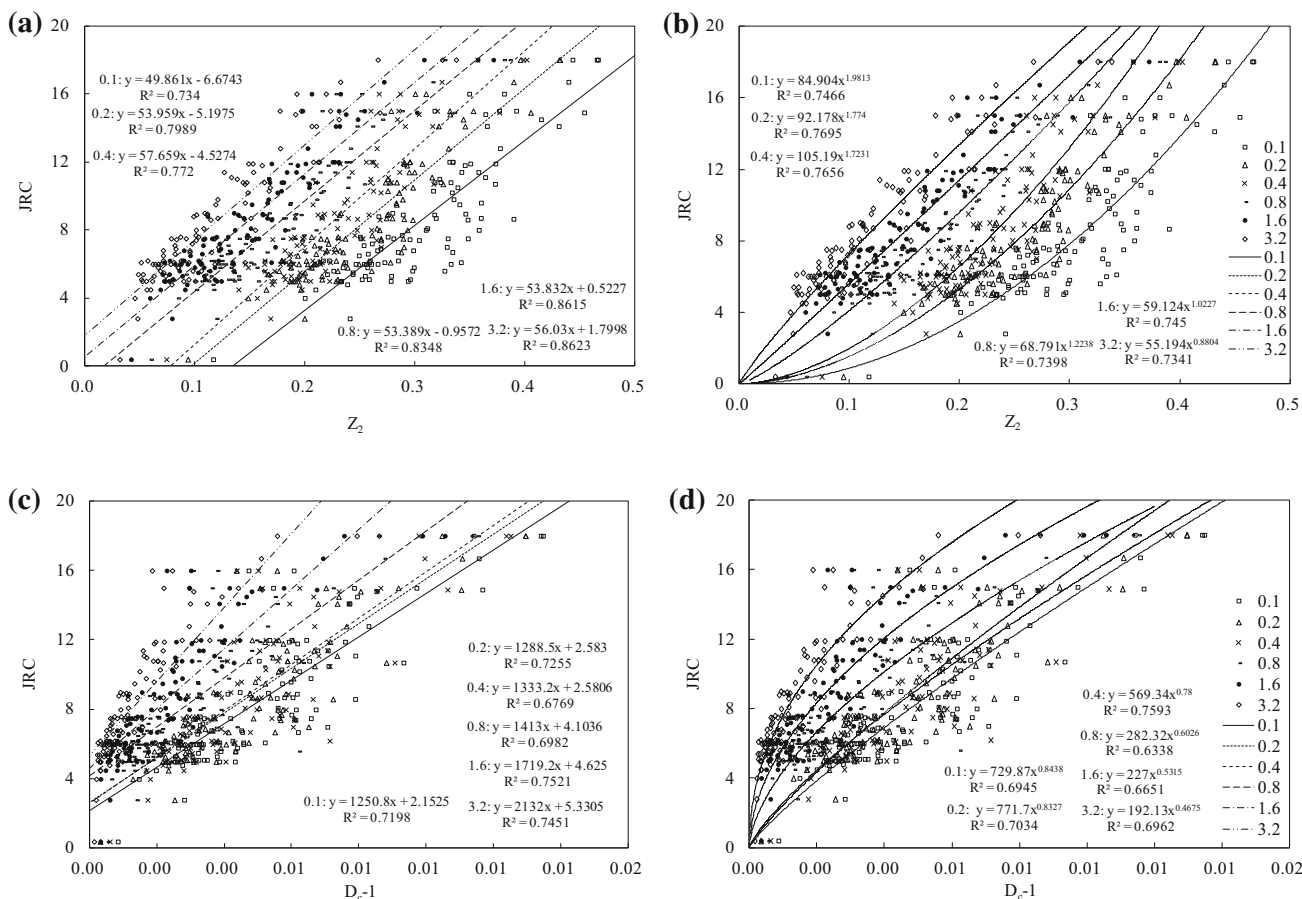


**Fig. 4** Influence of the sampling interval on Z<sub>2</sub>-estimates of JRC (a, b) and D<sub>c</sub>-estimates (c, d); a, c shows linear (y = ax + b) correlations; and b, d shows power-law (y = ax<sup>b</sup>) correlations

$$JRC = 4.6836R_z^{0.6106} (R = 0.8115) \tag{4}$$

$$JRC = 92.709(D_{h-L} - 1)^{0.377} (R = 0.8493) \tag{5}$$

**Validation of the proposed equations**

Twenty-three rock joint samples (120 mm × 120 mm), including slightly weathered and clean tension cracks (Fig. 6), are collected from a granite quarry and subjected to laboratory tests using a strain-controlled direct shear apparatus. The normal loading is set to 500 kPa and served by a hydraulic jack. The strain rate is set to 0.3 mm/min. Load transducers are used to measure shear forces. The normal and horizontal displacements are measured using linear variable differential transducers with a capacity of 100 mm and an accuracy of within ±0.1% of the indicated measurement. The data log system is equipped with the apparatus for recording shear displacement, shear force, normal force, and normal displacement. Figure 7 presents a shear stress versus shear displacement curve that was produced from a joint direct shear test. The joint wall

compressive strength (JCS) is obtained by a Schmidt hammer (Aydin 2009).

A simple yet efficient device is developed for estimating the JRC and peak shear strength of rock joints (Fig. 8). This device, patented by the National Patent Office of China, comprises two parts, namely, the main frame and the control and data analysis system. The main frame comprises a beam and three adjustable legs that maintain the stability of the device during operation. A handle for operating the device is installed on top of the beam. The beam and legs are made of aluminum alloy to reduce the weight of the device. A slider is driven by a motor that is mounted at the end of the beam using a guide screw. A laser sensor is mounted on the slider to measure the distance to the joint surface. The control and data analysis system adjusts the scanning speed and sampling frequency.

After scanning the joint surface, the control and data analysis system calculates the roughness parameters ( $\delta$ ,  $\sigma_i$ ,  $\lambda$ ,  $R_z$ , and  $D_{h-L}$ ), which are then used to calculate JRC with the correlations presented in Eqs. 1–5. The average JRC values from the five equations are used to calculate the peak shear strength of the rock joint according to the JRC–

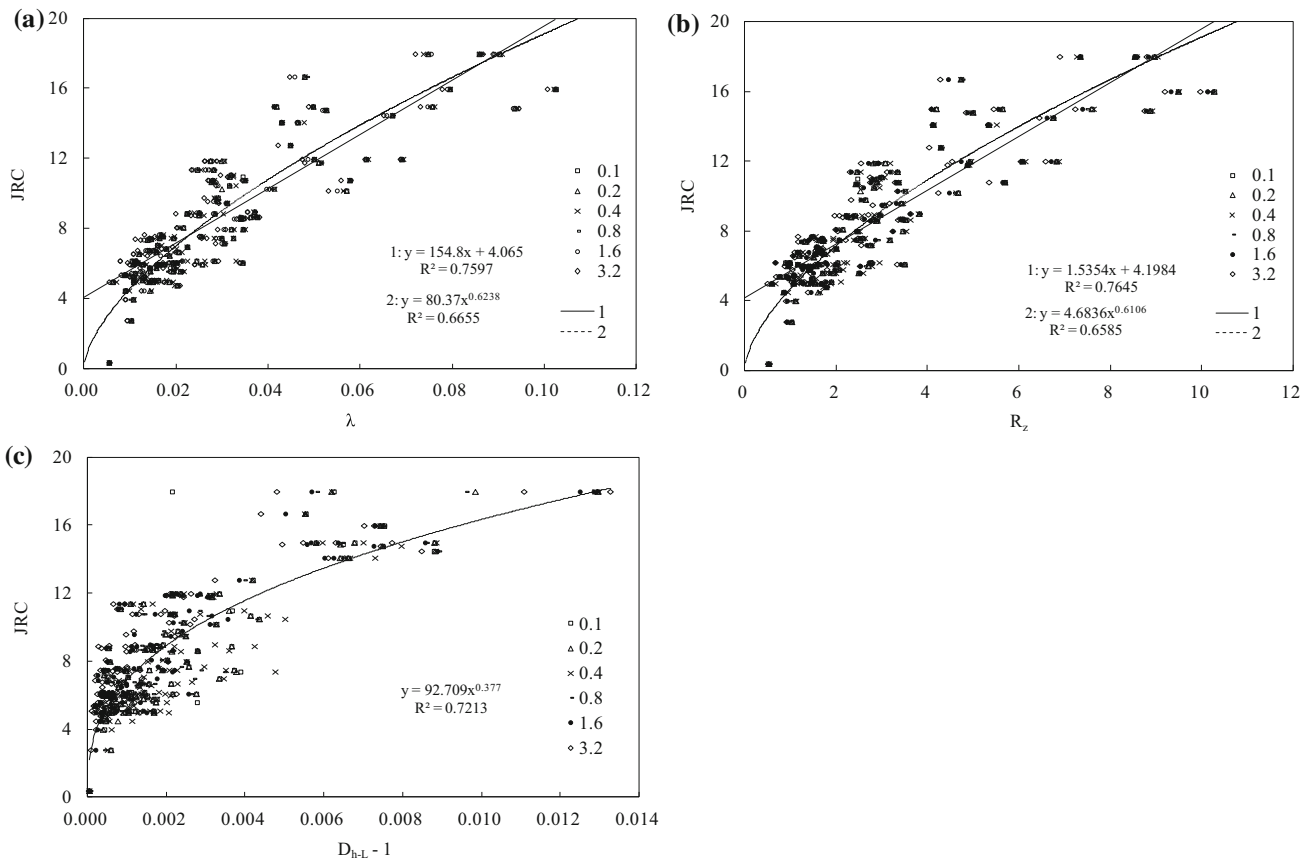


**Fig. 5** Independence of  $\lambda$ -,  $R_z$ -, and  $D_{h-L}$ -estimates of JRC on the sampling interval: **a** and **b** show both linear (solid line) and power-law (dashed line) correlations with good correlation coefficients.

**c** Shows only power-law correlation as there is no close linear correlation between  $D_{h-L} - 1$  and JRC

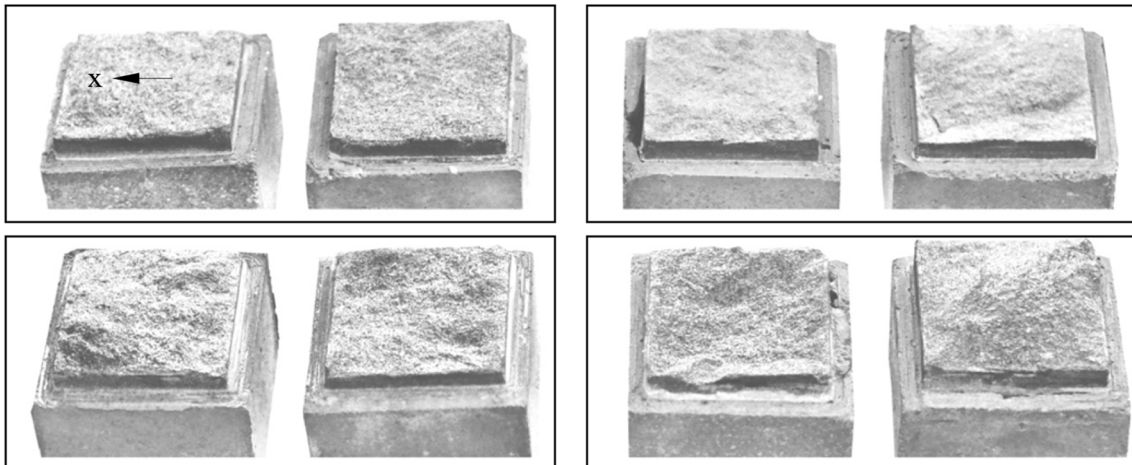


**Fig. 6** Tested samples with different roughness degrees. *x* indicates the shear direction

JCS model of Barton (1973). The basic friction angle, JCS, and normal stress ( $\sigma_n$ ) are inputted into the data analysis system for the calculation. The final results are displayed on the screen and stored in a flash memory card together with the raw scanning data.

The peak shear strengths of the prepared 23 samples as estimated by the newly developed device ( $\tau_e$ ) are compared with those estimated from the direct shear tests ( $\tau_t$ ). The relative error ( $\delta_e$ ) is calculated as  $\delta_e = |\tau_e - \tau_t|/\tau_t \times 100\%$ . As shown in Fig. 9a, the largest relative error between  $\tau_e$

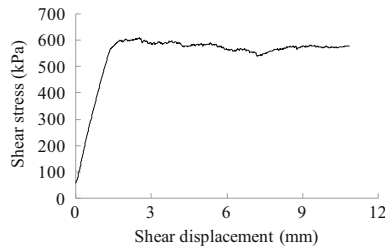


**Fig. 7** Example of direct shear test results given as a plot of shear stress vs. shear displacement

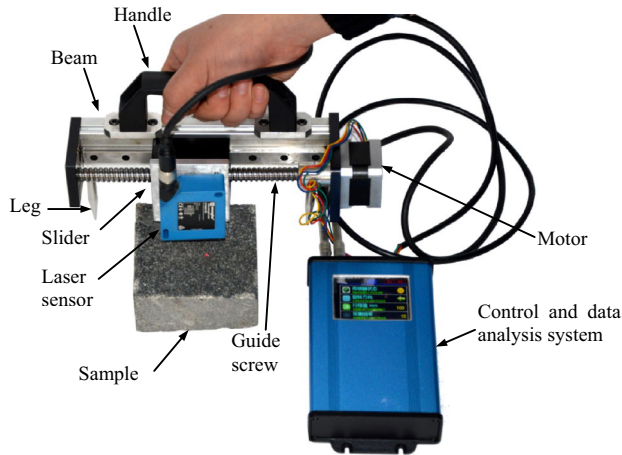


**Fig. 8** The rock joint shear strength estimation device in use on test specimens

and  $\tau_t$  was equal to 23%. Approximately 71% of the estimations are close to  $\tau_t$  with relative errors of less than 10%, while 88% of the estimations have relative errors of less than 15%. In sum, the proposed equations can provide a credible estimation of rock joint shear strength.

**Uncertainties in JRC estimates**

Although popular in engineering practice, the visual comparison approach suffers from subjectivity. The 111 rock

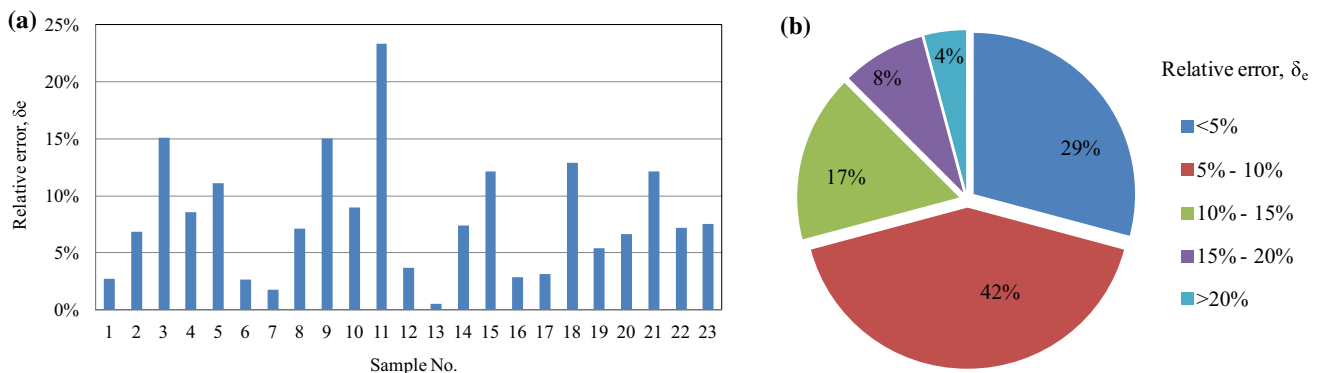
joint profiles in the second set (see “Data preparation”) are used to evaluate the uncertainties and errors in visual comparison. The  $JRC_e$  values of these profiles are estimated by Eqs. 1–5.

Figure 10 plots the statistical distribution of the deviation ( $\gamma = JRC_v - JRC_e$ ) of  $JRC_v$  from  $JRC_e$ . Figure 10a–e show similar distribution patterns, thereby indicating a fair consistency among the  $JRC_e$  values that are estimated using different empirical equations. Generally, the deviation of  $JRC_v$  from  $JRC_e$  exhibits a normal distribution with a mean of approximately  $-2.9$  regardless of the empirical equations used. The deviation ( $\gamma$ ) ranges from  $-15$  to  $8$ . Figure 11 shows that approximately 63.4% of the absolute errors ( $|y|$ ) are greater than 2, while 11.5% of these errors exceed 8.

The above observations indicate that (1) significant uncertainties can be introduced during visual comparison, and (2) visual comparison tends to generate smaller JRC values than the quantitative approaches using empirical equations. Those profiles with  $|y|$  values exceeding 6 were examined. The uncertainties or errors in the  $JRC_v$  values estimated by visual comparison could be attributed to the following:

*Main trend of the profile*

During data preparation, it is found that the best-fit lines through the 10 standard profiles are not horizontal, but have non-zero overall slopes. A similar case is observed for the remaining 213 profiles. Jia (2011) assigned a  $JRC_v$  of 11 to the profile in Fig. 12a, which bears the closest resemblance to the ISRM 10–12 profile in Fig. 12b. However, when plotted together as in Fig. 12c, these two profiles do not appear similar. After removing the main trend by the least square, the resultant profile resembles most to the ISRM 18–20 profile in Fig. 12d. This finding is consistent with the  $JRC_e$  value of 19.2. Tatone and Grasselli (2010) also suggested removing the main trend of the profile when estimating JRC.



**Fig. 9** Relative error between the estimates and the test-determined values of peak shear strength: **a** the relative error,  $\delta_e = |\tau_e - \tau_t|/\tau_t \times 100\%$ , and **b** percentage distribution of  $\delta_e$



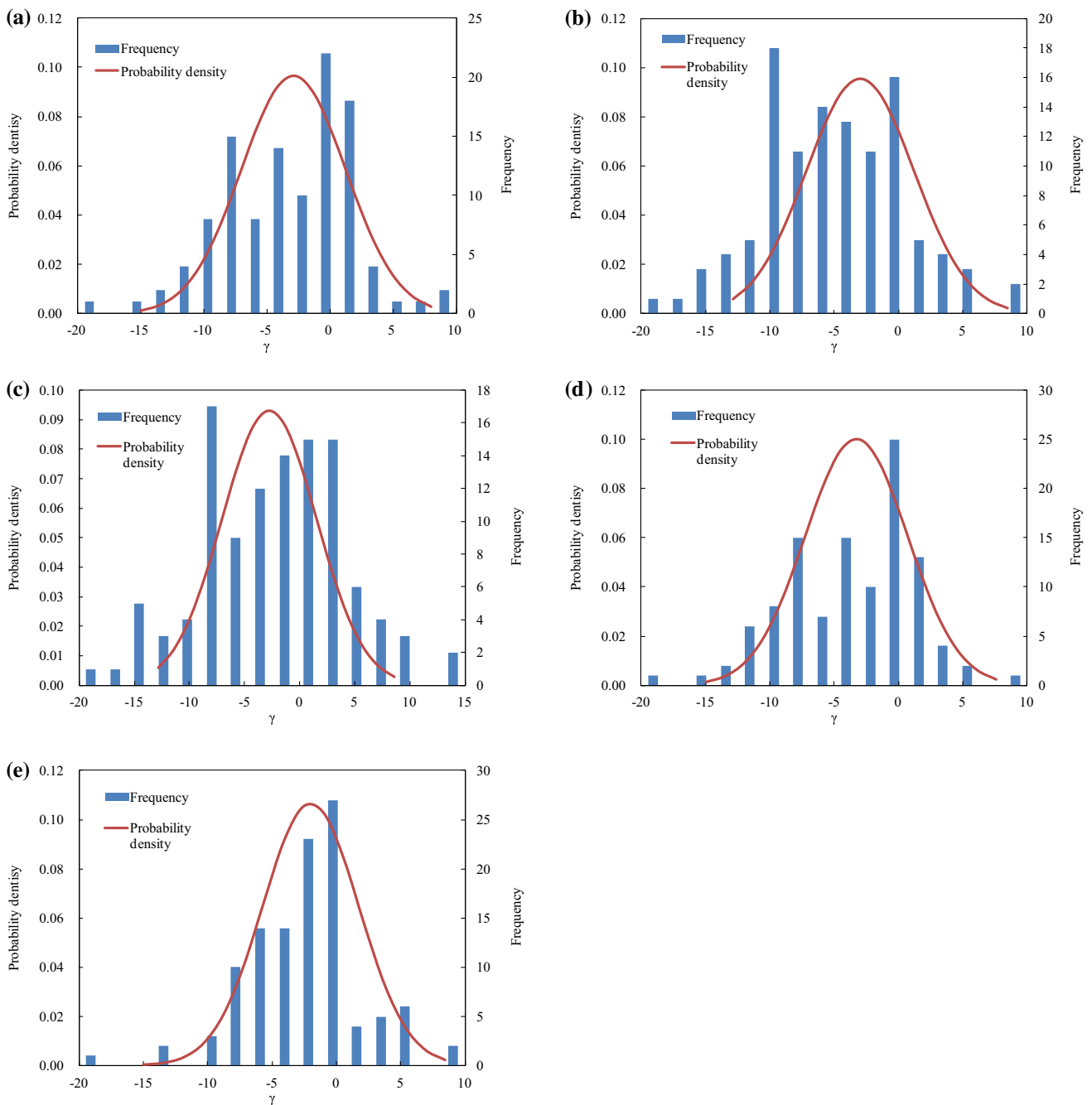


**Fig. 10** Statistical distributions of the deviation ( $\gamma$ ) of  $JRC_v$  from  $JRC_e$  derived from different parameters: **a**  $\sigma_i$ , **b**  $R_z$ , **c**  $\lambda$ , **d**  $\delta$ , and **e**  $D_{h-L}$

*Limitation of the standard set*

The limited scope of the standard set may also introduce errors in estimating JRC via visual comparison. As shown in Fig. 13a, b, the two profiles from Jia (2011) are apparently outside the scope of the Barton’s chart, which only contains 10 profiles. For a profile that is outside the scope of the standard set, the maximum height ( $R_z$ ) can be treated as a criterion when estimating JRC because of its easy application and strong correlation with JRC (Eq. 4).

In order to limit the potential errors in estimating JRC via visual comparison, the chart of the standard profiles is modified as given in Fig. 14. The modification involves realigning the profiles such that the best-fit linear regression line through each profile is horizontal, and adding a scale bar for the y-axis. The latter is provided to help remind that visual comparison require both profiles (the compared and the standard) must have identical vertical, as well as horizontal scales. The  $R_z$  can also be used to guide visual comparison when resemblance is not obvious.

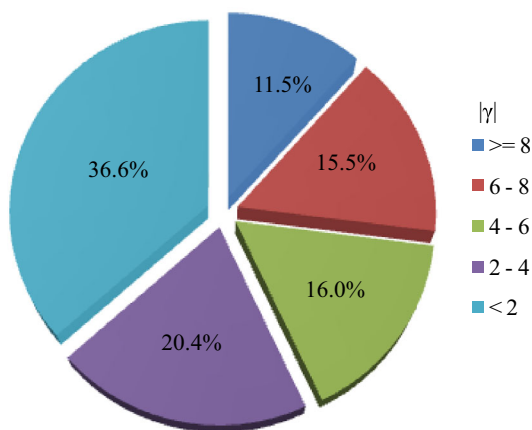


**Fig. 11** Percentage distribution of the absolute error ( $|\gamma|$ ) of  $JRC_v$  from  $JRC_e$

**Conclusions**

This study is based on 223 rock joint profiles retrieved from the literature. Of these profiles, 112 are used to investigate the uncertainties in quantitatively estimating JRC based on different SIs, while 111 are used to examine the uncertainties in visual estimation. The following conclusions are derived:

1. The quantitative correlations of JRC with the parameters  $Z_2$ ,  $\sigma_i$ ,  $\delta$ , and  $D_c$  are sensitive to the sampling interval, while those with  $R_z$ ,  $\lambda$ , and  $D_{h-L}$  are not. Consistent with these observed differences, this study proposes two separate sets of equations for quantitatively estimating JRC. The direct shear tests on 23 rock joint samples indicate that the proposed equations can provide credible estimations of the JRC and peak shear strength of

rock joints. Given that the proposed equations are derived from joint profiles that are digitized at SIs ranging from 0.1 to 3.2 mm, they must be cautiously applied for the data that fall outside this range.

2. The deviation of  $JRC_v$  (visual comparison) from  $JRC_e$  (quantitative approach) ranges from  $-15$  to  $8$ , and almost 64% of the absolute error values exceed 2. The deviation exhibits a normal distribution with an approximate mean of  $-2.9$ , indicating that the JRC values estimated via visual comparison are often underestimated. Such deviations are attributed to the presence of a non-horizontal main trend in the profile and to the limited scope of the standard profiles.
3. The chart of the standard profiles is updated by realigning each profile and adding a y-axis scale containing the maximum height in the profiles. When visually comparing a profile: (1) remove the main trend before the comparison; and (2) use the maximum height  $R_z$  of the profile as the main criterion if there is no obvious match with any of the standard profiles.

**Acknowledgements** This study is supported by the National Natural Science Foundation of China (No. 51309176). The authors thank Messrs. Mo, P. and He, S.D. for their help in preparing the data. The digital datasets can be provided to researchers upon request.

**Appendix**

The definition and calculation of some of the parameters used in this paper:  $Z_2$ : Root mean square of the first deviation of the profile (Tse and Cruden 1979)

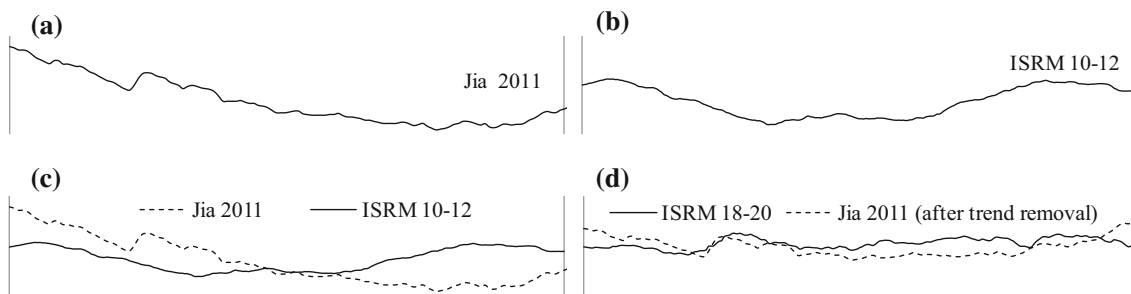


**Fig. 12** Error in estimation of JRC due to the presence of a non-horizontal main trend in the profile

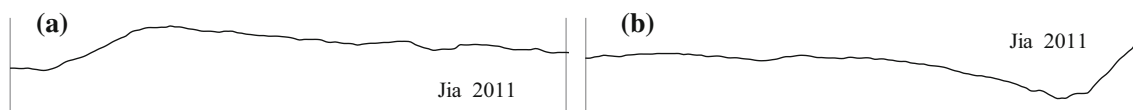
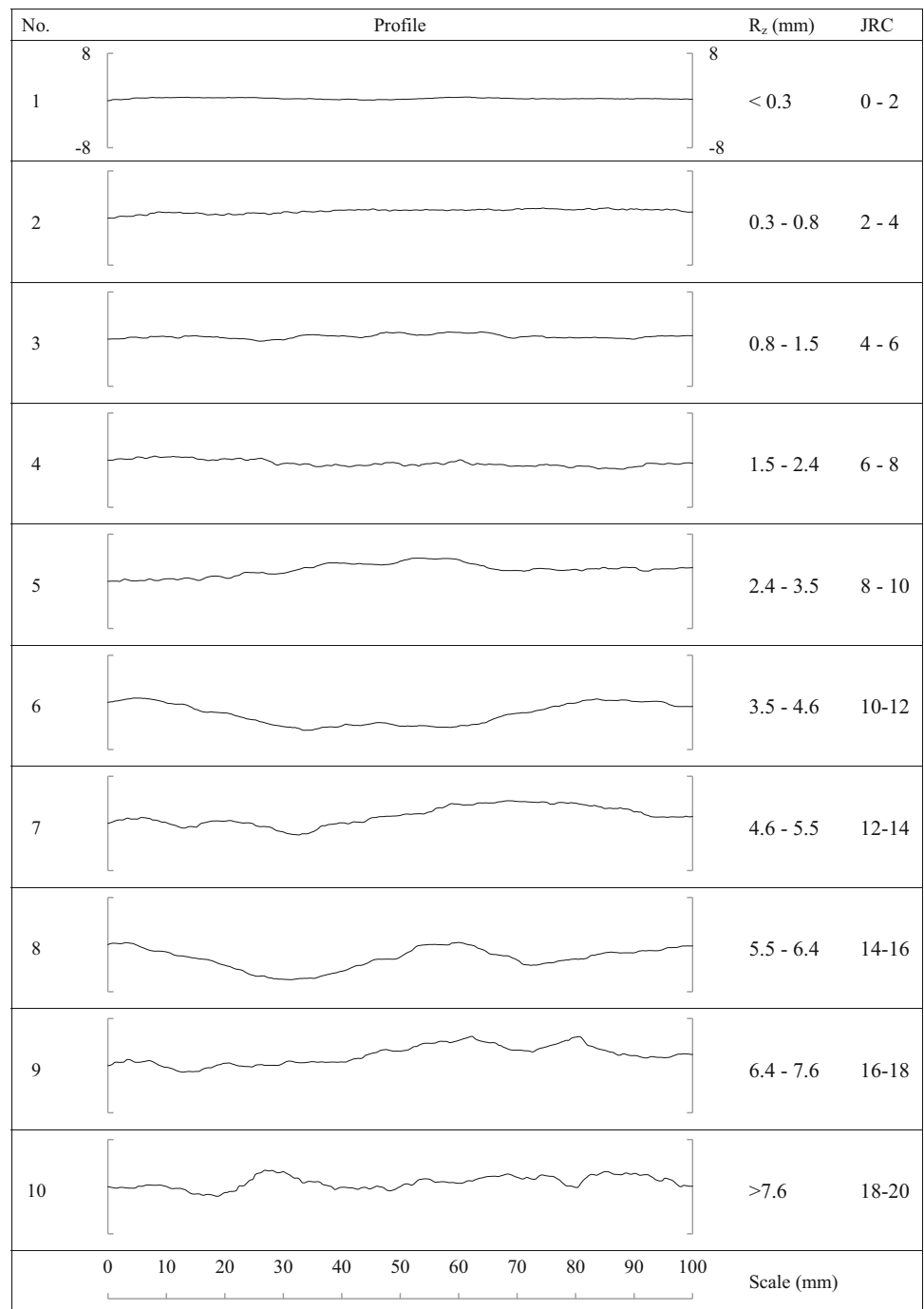


**Fig. 13** Examples of rock joint profiles beyond the scope of the ten standard profiles

**Fig. 14** Updated Barton’s chart with the standard profiles realigned to the horizontal



$$Z_2 = \left[ \frac{1}{L} \int_{x=0}^{x=L} \left( \frac{dy}{dx} \right)^2 dx \right]^{\frac{1}{2}} = \left[ \frac{1}{L} \sum_{i=1}^{N-1} \frac{(y_{i+1} - y_i)^2}{x_{i+1} - x_i} \right]^{1/2}$$

where  $dx$  is the increment of  $x$  of the profile;  $dy$  is the increment of  $y$  of the profile;  $N$  is the number of evenly spaced sampling points; and  $x_i$  and  $y_i$  are the  $x$ - and  $y$ -coordinates of sampling point.

$\sigma_i$ : Standard deviation of the angle  $i$  (Yu and Vayssade 1991)

$$\sigma_i = \tan^{-1} \left[ \frac{1}{L} \int_{x=0}^{x=L} \left( \frac{dy}{dx} - \tan i_{ave} \right)^2 dx \right]^{\frac{1}{2}}$$

$$i_{ave} = \frac{1}{L} \int_{x=0}^{x=L} \tan^{-1} \left( \frac{dy}{dx} \right) dx$$

$R_z$ : Maximum height of a profile, equals to the vertical distance between the highest peak and the lowest valley.

$L$ : The projected length of the profile

$$L = \sum_{i=1}^{N-1} (x_{i+1} - x_i).$$

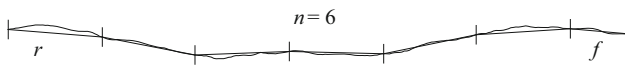
$\lambda$ : Ultimate slope of the profile,  $\lambda = R_z/L$ .

$\delta$ : Profile elongation index,  $\delta = (L_t - L)/L$  (Maerz et al. 1990)

$$L_t = \sum_{i=1}^{N-1} \sqrt{(x_{i+1} - x_i)^2 + (y_{i+1} - y_i)^2}$$

$D_c$ : Fractal dimension determined by compass-walking method (Maerz et al. 1990)

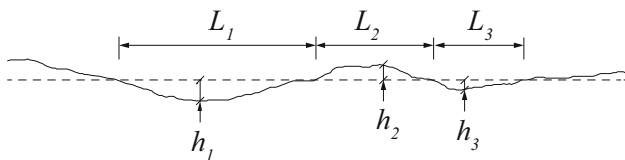
$$D = -\frac{\log(n + f/r)}{\log r}.$$



where  $n$  is the number of steps for walking through a joint profile by a divider with a span of  $r$ ; and  $f$  is the remaining length shorter than  $r$  after excluding the length of  $nr$ .

$D_{h-L}$ : Fractal dimension determined by the hypotenuse leg (h-L) (method (Li and Huang 2015))

$$D = \frac{\log 4}{\log[2(1 + \cos(\tan^{-1} \frac{2h}{l}))]} \quad (\text{where, } h = \frac{1}{M} \sum_{i=1}^M h_i \text{ and } l = \frac{1}{M} \sum_{i=1}^M L_i).$$



where  $l$  and  $h$  are the average base length and the average height of asperities of a joint, respectively; and  $M$  is the number of asperities.

## References

- Aydin A (2009) Suggested method for determination of the Schmidt hammer rebound hardness: Revised version. *Int J Rock Mech Min Sci* 46(3):627–634
- Bandis SC (1980) Experimental studies of scale effects on shear strength and deformation of rock joint. Ph.D. thesis, Univ. of Leeds, p 385
- Bandis SC, Lumsden AC, Barton NR (1983) Fundamentals of rock joint deformation. *Int J Rock Mech Min Sci Geomech Abstr* 6:249–268
- Barton N (1973) Review of a new shear-strength criterion for rock joints. *Eng Geol* 7:287–332
- Barton N, Choubey V (1977) The shear strength of rock joints in theory and practice. *Rock Mech* 10:1–54
- Beer AJ, Stead D, Coggan JS (2002) Estimation of the joint roughness coefficient (JRC) by visual comparison. *Rock Mech Rock Eng* 35(1):65–74
- Brown ET (1981) Rock characterization testing and monitoring (ISRM suggested methods). Pergamon Press, Oxford
- Carr JR, Warriner JB (1987) Rock mass classification of joint roughness coefficient. In: 28th US Symp on Rock Mechanics. Tucson, pp 72–86
- Du SG (1995) Mathematical expression of JRC modified straight edge. *J Eng Geol* 4(2):36–43 (in Chinese)
- Gao Y, Wong LNY (2015) A modified correlation between roughness parameter Z2 and the JRC. *Rock Mech Rock Eng* 48(1):387–396
- Grasselli G (2001) Shear strength of rock joints based on quantified surface description. PhD thesis, Ecole Polytechnique Federale De Lausanne (EPFL), p 124
- Grasselli G, Egger P (2003) Constitutive law for the shear strength of rock joints based on three-dimensional surface parameters. *Int J Rock Mech Min Sci* 40(1):25–40
- Herda HHW (2006) An algorithmic 3D rock roughness measure using local depth measurement clusters. *Rock Mech Rock Eng* 39(2):147–158
- Jia HQ (2011) Experimental research on joint surface state and the characteristics of shear failure. MSc. thesis, Central South University, Changsha China, p 78 (in Chinese)
- Kulatilake PHSW, Shou G, Huang TH, Morgan RM (1995) New peak shear strength criteria for anisotropic rock joints. *Int J Rock Mech Min Sci Geomech Abstr* 32(7):673–697
- Lee YH, Carr JR, Bars DJ, Hass CJ (1990) The fractal dimension as a measure of the roughness of rock discontinuity profiles. *Int J Rock Mech Min Sci Geomech Abstr* 27(6):453–464
- Li YR, Huang RQ (2015) Relationship between joint roughness coefficient and fractal dimension of rock fracture surfaces. *Int J Rock Mech Min Sci* 75:15–22
- Li YR, Zhang YB (2015) Relationship between joint roughness coefficient and statistical parameters of rock fracture surfaces. *Int J Rock Mech Min Sci* 77:27–35
- Maerz NH, Franklin JA, Bennett CP (1990) Joint roughness measurement using shadow profilometry. *Int J Rock Mech Min Sci Geomech Abstr* 27:329–343
- Odling NE (1994) Natural fracture profiles, fractal dimension and joint roughness coefficients. *Rock Mech Rock Eng* 27(3):135–153
- Rasouli V, Hosseinian A (2011) Correlations developed for estimation of hydraulic parameters of rough fractures through the simulation of JRC flow channels. *Rock Mech Rock Eng* 44:447–461
- Seidel JP, Haberfield CM (1995) The application of energy to the determination of the sliding resistance of rock joints. *Rock Mech Rock Eng* 24(4):211–226
- Tatone BSA (2009) Quantitative characterization of natural rock discontinuity roughness in situ and in the laboratory. MAsc. thesis, University of Toronto, Toronto. <http://hdl.handle.net/1807/18959>
- Tatone BSA, Grasselli G (2010) A new 2D discontinuity roughness parameter and its correlation with JRC. *Int J Rock Mech Min Sci* 47:1391–1400
- Tatone BSA, Grasselli G (2013) An investigation of discontinuity roughness scale dependency using high-resolution surface measurements. *Rock Mech Rock Eng* 46:657–681
- Tse R, Cruden DM (1979) Estimating joint roughness coefficients. *Int J Rock Mech Min Sci Geomech Abstr* 16:303–307
- Turk N, Greig MJ, Dearman WR, Amin FF (1987) Characterization of joint surfaces by fractal dimension. In: 28th US Symp on Rock Mechanics, Tucson, pp 1223–1236

- Vladimir G, Tomas D (2011) Stanovenie koeficienta drsnosti pulin (JRC) metodou blizkej digitalnej fotogrametrie. *Acta Geol Slovaca* 3(2):163–172
- Wang Q (1982) Study on determination of rock joint roughness by using elongation rate R. *Proc. Underg. Constr, Jinchuan*, pp 343–348
- Xie HP, Pariseau WG (1994) Fractal estimation of rock joint roughness coefficient. *Sci China (Ser B)* 24(5):524–530
- Yang ZY, Lo SC, Di CC (2001) Reassessing the joint roughness coefficient (JRC) estimation using Z2. *Rock Mech Rock Eng* 34:243–251
- Yu XB, Vayssade B (1991) Joint profiles and their roughness parameters. *Int J Rock Mech Min Sci Geomech Abstr* 28:333–336
- Zhang GC, Karakus M, Tang HM, Ge YF, Zhang L (2014) A new method estimating the 2D joint roughness coefficient for discontinuity surfaces in rock masses. *Int J Rock Mech Min Sci* 72:191–198